Testing Hardy's nonlocality proof with genuine energy-time entanglement

Giuseppe Vallone,[1,2] Ilaria Gianani,[2] Enrique B. Inostroza,[3,4] Carlos Saavedra,[3,4] Gustavo Lima,[3,4,*] Adán Cabello,[5] and Paolo Mataloni[2,6]

[1]*Museo Storico della Fisica e Centro Studi e Ricerche "Enrico Fermi", Via Panisperna 89/A, Compendio del Viminale, Roma I-00184, Italy*

[2]*Dipartimento di Fisica, Università Sapienza di Roma, I-00185 Roma, Italy*

[3]*Center for Optics and Photonics, Universidad de Concepción, Casilla 4016, Concepción, Chile*

[4]*Departamento de Física, Universidad de Concepción, Casilla 160-C, Concepción, Chile*

[5]*Departamento de Física Aplicada II, Universidad de Sevilla, E-41012 Sevilla, Spain*

[6]*Istituto Nazionale di Ottica, Consiglio Nazionale delle Ricerche (INO-CNR), Largo E. Fermi 6, I-50125 Firenze, Italy*

(Received 26 January 2011; published 18 April 2011)

We show two experimental realizations of Hardy's ladder test of quantum nonlocality using energy-time correlated photons, following the scheme proposed by Cabello *et al.* [Phys. Rev. Lett. **102**, 040401 (2009)]. Unlike previous energy-time Bell experiments, these tests require precisely tailored nonmaximally entangled states. One of them is equivalent to the two-setting and two-outcome Bell test requiring a minimum detection efficiency. The reported experiments are still affected by the locality and detection loopholes, but are free of the post-selection loophole of previous energy-time and time-bin Bell tests.

DOI: 10.1103/PhysRevA.83.042105 PACS number(s): 03.65.Ud, 03.67.Mn, 42.50.Xa

I. INTRODUCTION

A loophole-free violation of a Bell inequality would prove the impossibility of describing nature in terms of local hidden-variable theories [1], and the possibility of post-quantum secure communications [2]. Among all versions of Bell's proof, Hardy's [3,4] is one of the simplest. In addition to simplicity, Hardy's version has one interesting feature: it only works for nonmaximally entangled states, which are precisely the best candidates for a photonic loophole-free experiment with inefficient detectors [5,6]. To be more specific, the experimental realization of the two-party, two-setting, and two-outcome Bell test with minimum required detection efficiency, assuming that all detectors have the same efficiency [5,6], is equivalent to a test of Hardy's proof.

Standard energy-time and time-bin Bell tests (e.g., Ref. [7]) suffer from a specific loophole called the post-selection loophole [8,9], which can be avoided using a scheme introduced in Ref. [9]. Energy-time Bell experiments with maximally entangled states and free of the post-selection loophole have been recently performed by using this scheme [10]. Moreover, the scheme can be applied to nonphotonic systems [11] and can be extended to multipartite scenarios [12].

The aim of this work is to show that energy-time entanglement can also be used to produce Hardy-type violations of Bell inequalities free of the post-selection loophole, as a preliminary step toward a loophole-free Bell test with photonic random destination sources [13]. The two experiments reported in this paper will also show the feasibility of energy-time entanglement for producing nonmaximally entangled states, which are essential for some quantum-key-distribution protocols [14].

II. HARDY'S PROOF

Hardy's proof of nonlocality [3,4] can be summarized as follows. Let us consider two observers, Alice and Bob, measuring dichotomic (with outputs -1 and 1) observables. Alice measures a_0 and a_1, while Bob measures b_0 and b_1. Let us define $P(a_i,b_j)$ as the joint probability of obtaining $a_i = b_j = 1$, and $P(\bar{a}_i,b_j)$ as the joint probability of obtaining $a_i = -1$ and $b_j = 1$. For any local hidden-variable theory with (i) $P(a_0,b_0) = 0$, (ii) $P(\bar{a}_0,b_1) = 0$, and (iii) $P(a_1,\bar{b}_0 = 0)$, the probability $P(a_1,b_1)$ must be equal to zero. However, for any nonsymmetric pure entangled state, it is always possible to find observables a_0, a_1, b_0, and b_1 such that (i), (ii), and (iii) are satisfied while (iv) $P(a_1,b_1) \neq 0$ [15]. $P(a_1,b_1)$ is known as the "Hardy fraction." This provides a proof of the impossibility of describing quantum mechanics with local hidden-variable theories.

As shown by Garuccio and Mermin [16,17], Hardy's proof can be put in a more generalized framework by writing it in terms of the following inequality:

$$\mathcal{S}_1 \equiv P(a_1,b_1) - P(a_0,b_0) - P(\bar{a}_0,b_1) - P(a_1,\bar{b}_0) \leqslant 0, \tag{1}$$

which holds for any local hidden-variable theory, for any choice of observables. In this generalized version, there is no need for vanishing terms in the experimental test; it is only required that $P(a_1,b_1)$ overcomes the sum of the remaining probabilities of Eq. (1). Nevertheless, the interesting feature of Hardy's argument lies in the fact that once one has proven that the probabilities on the right-hand side of the Garuccio-Mermin inequality are null, the detection of just one pair of photons, at the output $a_1 = 1$ and $b_1 = 1$, is enough to refute the local behavior of nature. However, under realistic conditions, measuring a null probability is not trivial, as discussed in Ref. [16], and the generalization of Hardy's test to the Bell-type test based on the Clauser-Horne (CH) inequality [18] is unavoidable.

The inequality given in Eq. (1) is the CH inequality for an experiment where the following conditions hold: (a) The

*glima@udec.cl

quantum efficiency of the detectors is $\eta = 1$ and (b) photon pairs impinge into the detection apparatuses. Therefore, Hardy's proof can be seen as a special case of a Bell test based on the CH inequality. This can be easily demonstrated. By taking into account the above detection conditions, the resulting probabilities of single-photon detections are given by

$$P_A(a_i) = P(a_i,b_j) + P(a_i,\bar{b}_j), \tag{2a}$$
$$P_B(b_j) = P(a_i,b_j) + P(\bar{a}_i,b_j), \tag{2b}$$

with $i = 0,1$ and $j = 0,1$. For the experimental setup being considered, the CH inequality can be written as

$$P(a_1,b_1) + P(a_0,b_1) + P(a_1,b_0) - P(a_0,b_0) - P_A(a_1) - P_B(b_1) \leqslant 0, \tag{3}$$

which becomes Eq. (1) when one replaces the marginal probabilities of Eq. (2b) into Eq. (3). It is also worth mentioning that under these conditions, the CH inequality is equivalent to the Clauser-Horne-Shimony-Holt (CHSH) inequality [19]. Therefore, Hardy's proof can also be seen as a particular case of the nonlocality tests based on the CHSH inequality. Indeed, any experimental setup prepared for testing the CHSH inequality can also be used to test Hardy's proof if the degree of entanglement of the state being generated can be manipulated.

Hardy's proof can be generalized by considering a system in which, having defined $K+1$ dichotomic observables a_k and b_k $(k = 0,\ldots,K)$, the following probabilities hold:

$$\left.\begin{aligned} &P(a_K,b_K) \neq 0,\\ &P(\bar{a}_{k-1},b_k) = 0,\\ &P(\bar{a}_k,b_{k-1}) = 0. \end{aligned}\right\} \quad k = 1,\ldots,K. \tag{4}$$

When K is larger than 1, the test can be interpreted as a chained violation and represented as a ladder [20,21] on which each step implies the one below (see Fig. 1).

Let us consider, for example, $K = 2$. If the first equation in (4) holds, then there exists a nonzero probability that both $a_2 = 1$ and $b_2 = 1$ occur. The second and third equations in (4) state that the probabilities of $a_2 = 1$ and $b_1 = -1$, or $a_1 = -1$ and $b_2 = 1$, are zero. In this case, $a_1 = 1$ and $b_1 = 1$ should have been observed. The same applies to the lower step, reaching in this way the bottom of the ladder. At this point, we obtain that both $a_0 = 1$ and $b_0 = 1$ should have been measured, and thus the probability $P(a_0,b_0)$ should be different from zero. In local theories, $P(a_0,b_0)$ should be at least equal to $P(a_K = 1,b_K = 1)$. If there exists a system in which this probability is vanishing, a classical theory would not be able to describe the system, and the Hardy inequality would be violated. A system like that can be implemented by the setup shown in the next section. It can be tested by generalizing Eq. (1) for the ladder proof case as

$$\mathcal{S}_K \equiv P(a_K,b_K) - P(a_0,b_0) - \sum_{k=1}^{K}[P(a_k,\bar{b}_{k-1}) + P(\bar{a}_{k-1},b_k)] \leqslant 0. \tag{5}$$

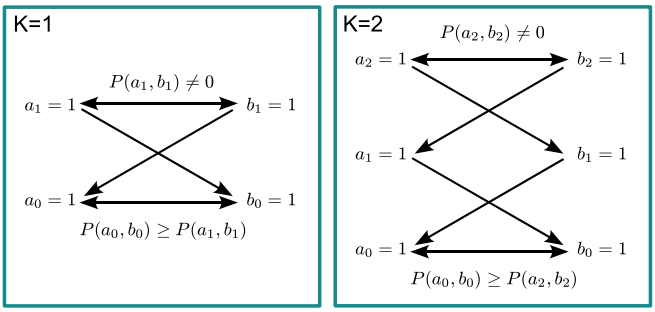

FIG. 1. (Color online) Ladder proof schemes for $K = 1$ and $K = 2$.

III. EXPERIMENT

A. Energy-time Hardy's test

A Hardy's test can be, in principle, implemented by using any entangled state, except the one which is maximally entangled. Our capacity to generate two photons correlated in the energy-time degree of freedom in partially entangled states, and the ability to detect them with controllable interferometric techniques, allows for implementing a Hardy's test with the experimental setup of Fig. 2. Let us consider the energy-time state of two down-converted photons $|\Phi\rangle \equiv \alpha|S_A S_B\rangle + \beta|L_A L_B\rangle$ and define the following $K+1$ spatial measurement basis, in each direction A_k and B_k, where $k = 0,\ldots,K$:

$$|A_k\rangle = \cos\theta_k|S\rangle + \sin\theta_k|L\rangle, \tag{6a}$$
$$|A_k^{\perp}\rangle = \sin\theta_k|S\rangle - \cos\theta_k|L\rangle, \tag{6b}$$
$$|B_k\rangle = \cos\theta_k|S\rangle + \sin\theta_k|L\rangle, \tag{6c}$$
$$|B_k^{\perp}\rangle = \sin\theta_k|S\rangle - \cos\theta_k|L\rangle. \tag{6d}$$

Let us define the operators a_k (b_k is defined similarly) as having outcome 1 or -1 when the state $|A_k\rangle$ or $|A_k^{\perp}\rangle$, respectively, is detected. In order to prove nonlocality, the conditions written in (4) must be satisfied. That is,

$$P(a_K,b_K) = |\langle A_K|\langle B_K|\Phi\rangle|^2 \neq 0, \tag{7a}$$
$$P(\bar{a}_{k-1},b_k) = |\langle A_{k-1}^{\perp}|\langle B_k|\Phi\rangle|^2 = 0, \tag{7b}$$
$$P(a_k,\bar{b}_{k-1}) = |\langle A_k|\langle B_{k-1}^{\perp}|\Phi\rangle|^2 = 0. \tag{7c}$$

Moreover, the following condition must hold:

$$P(a_0,b_0) = |\langle A_{k-1}^{\perp}|\langle B_{k-1}^{\perp}|\Phi\rangle|^2 = 0. \tag{8}$$

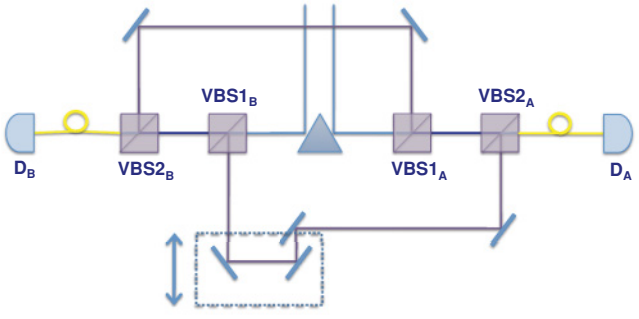

FIG. 2. (Color online) Scheme needed to implement a Hardy's test using energy-time entanglement. VBS: variable beam splitter.

The values of θ_k solving the previous equations are given by the relations

$$\sin\theta_k = (-1)^k \frac{T^{k+\frac{1}{2}}}{\sqrt{T^{2k+1}+1}}, \tag{9}$$

with $t = \alpha/\beta$ related to the degree of entanglement. The Hardy fraction $P(a_K,b_K)$ is then given by

$$P(a_K,b_K) = \frac{t^2(t^{2K}-1)^2}{(t^{2K+1}+1)^2(1+t^2)}. \tag{10}$$

When $K=1$ ($K=2$), this function is maximized at $t = t_1^* \simeq 0.46$ ($t = t_2^* \simeq 0.57$) with value $P(a_1,b_1)_{\max} \simeq 0.09$ [$P(a_2,b_2)_{\max} \simeq 0.17$]. When $K=1$, only 9% of particles violate locality, but this fraction can be amplified using a higher value of K. It has been shown, in fact, that when $K \longrightarrow \infty$, $P(a_K,b_K)_{\max} \longrightarrow 50\%$ [20].

B. Experimental setup

We generated energy-time correlated photons by spontaneous parametric down-conversion (SPDC) [22,23]. A 1-mm β-barium borate crystal (BBO) shined by a uv laser beam generated pairs of photons at a wavelength of 532 nm. The emission time of each pair is unpredictable due to the long coherence length ($\geqslant$1 m) of the pump laser beam. The two photons generated with horizontal polarization are sent through two unbalanced interferometers as shown in Fig. 3. As discussed below, this is a modified version of the interferometric scheme previously used by us [10]. As for the setup previously used, the geometry of these interferometers has been shown to allow for more genuine tests of quantum nonlocality with energy-time correlated photons [9]. In this case, even though the experiment is still constrained by the locality and detection loopholes [24], it is not necessary to assume any other auxiliary assumption for validating it as a conclusive Bell test [1]. These interferometers are unbalanced and so one can refer to their arms as short (S) and long (L). The optical paths followed by the down-converted photons are such that coincidences between detectors D_A and D_B are measured only when they both propagate through the short or long photon paths.

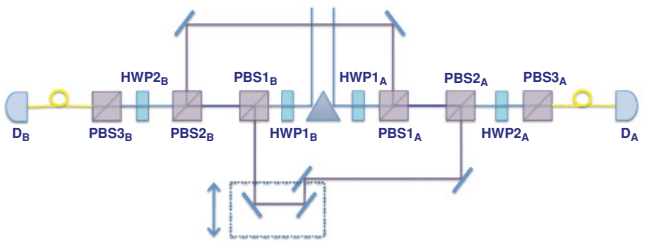

FIG. 3. (Color online) Experimental setup. A step-by-step translation stage allows us to create the indistinguishability condition ($L_A - S_A = L_B - S_B$). Coincidence windows are 3ns and, due to continuous wave pumping, the probability of two photon-pair events is negligible. Interference filters select a bandwidth of 3.5 nm. The radiation is coupled into single-mode optical fibers and sent to pigtailed avalanche photo-counting modules connected to a circuit used to record the single and the coincidence counts. The phase of the interferometer can be controlled using a piezoelectric stage on which PBS2$_A$ is assembled.

In order to perform a Hardy's test, nonmaximally entangled states are needed, and it is also possible to use just two detectors instead of four as used in the previous experiment [10]. The new scheme is shown in Fig. 2, where variable beam splitters (VBS1$_{A,B}$) are used on both modes in order to prepare the nonmaximally entangled state,

$$|\psi\rangle = \alpha|S_A S_B\rangle + \beta|L_A L_B\rangle. \tag{11}$$

In this way, the ratio $t = \alpha/\beta$ can be controlled by using the following relation between the transmittivities (T_A and T_B) and reflectivities (R_A and R_B) of VBS1$_{A,B}$ and t:

$$\sqrt{\frac{T_A T_B}{R_A R_B}} = \frac{\alpha}{\beta} = t. \tag{12}$$

The two VBS2$_{A,B}$ can be used to project into the states of Eqs. (6a)–(6d), providing that their transmittivities and reflectivities are linked to θ_k being $\sqrt{R} = \sin\theta_k$ and $\sqrt{T} = \cos\theta_k$.

In Fig. 3 we show the setup we actually used for the experiment. It is equivalent to the one shown in Fig. 2, but it does not use variable beam splitters.

The VBSs used to prepare the state, namely VBS1$_{A,B}$, are implemented in the way shown by the scheme of Fig. 4(a), where the polarization of both photons A and B is changed by a half-wave plate (HWP1), and then each photon is split in the long and short paths by a polarizing beam splitter (PBS1). After the PBS1, we will have on each mode, in transmission, the state $|S\rangle|H\rangle$, while on reflection, the state $|L\rangle|V\rangle$. By rotating HWP1, one can change the amount of light being reflected and transmitted, allowing the creation of a nonmaximally entangled state.

To implement the two VBS2, we used the scheme reported in Fig. 4(b): since the $|S\rangle$ ($|L\rangle$) mode is horizontally (vertically) polarized, any state encoded into the energy-time degree of freedom is converted into polarization encoding by the PBS2. Then the projection on the desired state can be implemented by the standard polarization analyzer (HWP2 rotated at $\theta_k/2$ and PBS3).

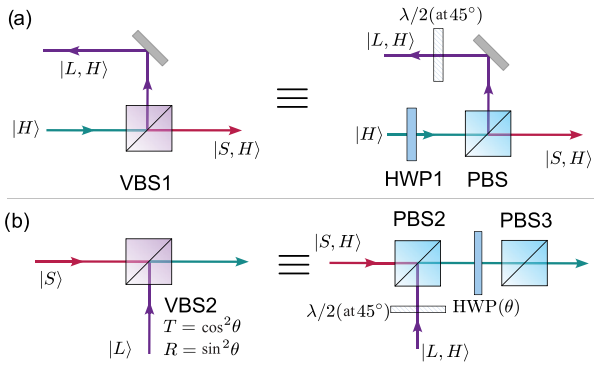

FIG. 4. (Color online) (a) Generation of nonmaximally entangled state and (b) projection on the measurement basis. This setup is repeated on both modes A and B, and is used to generate a nonmaximally entangled state and project on the desired base, as described in the text.

TABLE I. Experimental probabilities needed to violate the inequality $\mathcal{S}_K \leqslant 0$ for $K = 1$ and $K = 2$. The reported data are obtained with the value of t that maximizes the violation, namely, $t = t_1^* \simeq 0.46$ for $K = 1$, and $t = t_2^* \simeq 0.57$ for $K = 2$.

$K = 1, t = t_1^*$		$K = 2, t = t_2^*$	
$P(a_1,b_1)$	0.095 ± 0.005	$P(a_2,b_2)$	0.170 ± 0.008
$P(a_1,\bar{b}_0)$	0.005 ± 0.001	$P(a_2,\bar{b}_1)$	0.007 ± 0.002
$P(\bar{a}_0,b_1)$	0.005 ± 0.001	$P(\bar{a}_1,b_2)$	0.009 ± 0.002
$P(a_0,b_0)$	0.007 ± 0.001	$P(a_1,\bar{b}_0)$	0.009 ± 0.002
$\mathcal{S}_1$	0.078 ± 0.005	$P(\bar{a}_0,b_1)$	0.009 ± 0.002
		$P(a_0,b_0)$	0.011 ± 0.002
		$\mathcal{S}_2$	0.124 ± 0.009

C. Experimental results

Our experiment focused on the violation of the Hardy inequality (5) for $K = 1$ and $K = 2$. For this purpose, we measured the probabilities described by Eqs. (7) and (8) as

$$P = \frac{C(a_i = \alpha, b_j = \beta)}{C_{\mathrm{TOT}}}, \tag{13}$$

where i, j are the directions required, and $\alpha = \pm 1$ and $\beta = \pm 1$ as previously specified. $C(a_i = \alpha, b_j = \beta)$ is the number of coincidences obtained by measuring on the projected state needed for both modes, while $C_{\mathrm{TOT}} = C(H,H) + C(V,V) + C(H,V) + C(V,H)$ is the sum of the number of coincidences over all the possible outcomes in the base $\{|H\rangle, |V\rangle\}$.

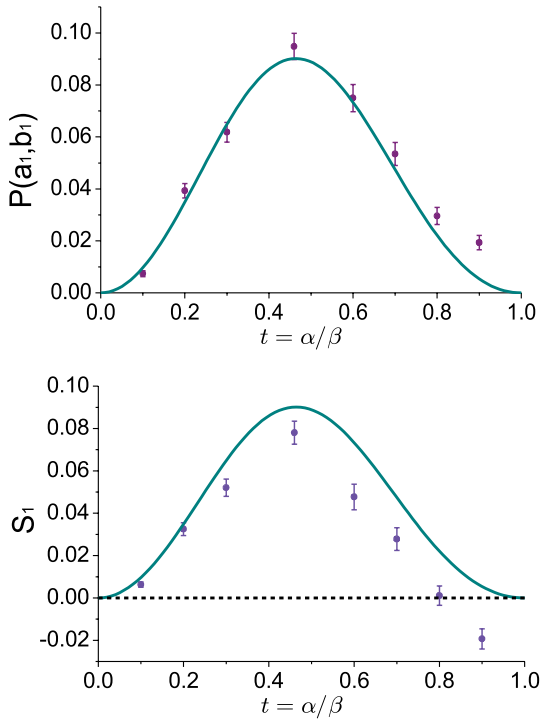

FIG. 5. (Color online) Experimental results for $K = 1$. These two graphs show the result obtained for the one-step ladder proof. The top graph shows the agreement between the data and the theoretical prediction (continuous line) for the probability $P(a_1,b_1)$. The bottom graph shows the obtained values of $\mathcal{S}_1$ compared to the theory (continuous line). The dotted line represents the classical bound: when $\mathcal{S}_1$ is greater than 0, the inequality (1) is violated.

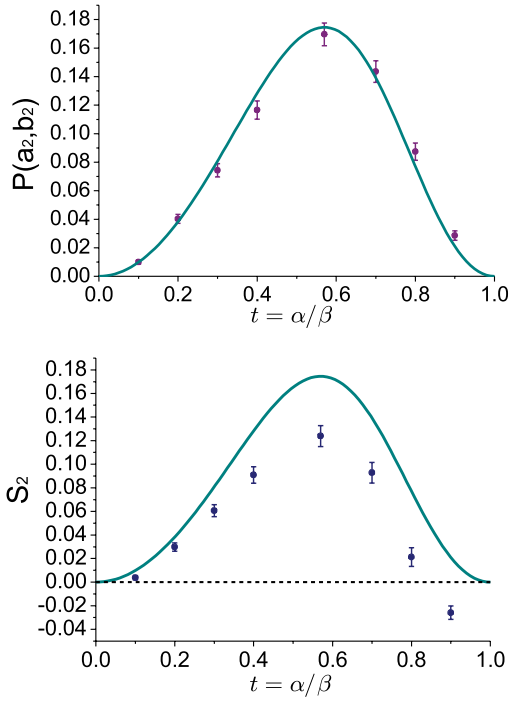

FIG. 6. (Color online) Experimental results for $K = 2$. The results obtained for a two-step ladder proof are shown. As in the previous figure, the top graph shows the probability $P(a_2,b_2)$ along with the theoretical function, while the bottom graph shows the inequality violation. When $\mathcal{S}_2$ is greater than 0, the inequality (5) is violated.

In Table I, we show the experimental probabilities obtained for $K = 1$ and $K = 2$ when $t = t_1^*$ and $t = t_2^*$, respectively. In Figs. 5 and 6 we show the probabilities obtained for $K = 1$ and $K = 2$ for different values of $t = \alpha/\beta$. Each figure shows the graph of the experimental $P(a_K,b_K)$ compared to the theoretical values described by Eq. (10) and the graph of the inequality violation $\mathcal{S}_K$ defined in (1) and (5). The obtained values of $P(a_K,b_K)$ are in good agreement with the theoretical predictions for both K values. The inequality is not violated for large values of t, where $t \geqslant 0.8$ (see Figs. 5 and 6). This can be due to the imperfect experimental visibility. In fact, we measured $V \sim 96\%$ when the state is maximally entangled ($t = 1$). However, this value is not enough to allow the probabilities $P(a_k,\bar{b}_{k-1})$, $P(\bar{a}_{k-1},b_k)$, and $P(a_0,b_0)$ to vanish completely. This feature is more evident when the degree of entanglement increases since, in this case, the $|SS\rangle/|LL\rangle$ interference is more important.

IV. CONCLUSIONS

Recently introduced schemes for energy-time and time-bin entanglement can be improved for a Bell test with nonmaximally entangled states free of the post-selection loophole. The important point is that these tests are less demanding in terms of detection efficiency than those based on maximally entangled states (which were the states used in previous Bell tests with energy-time and time-bin entanglement), even when the post-selection is taken into account [13]. The experiments reported in this paper still suffer the detection and nonlocality loopholes, but show the feasibility of energy-time Bell tests

with nonmaximally entangled states and free of the post-selection loophole.

In addition, the ability to project energy-time correlated photons in this more general set of projections may also have other important applications. It could be useful for entanglement witnesses, quantum tomography, and some cryptographic protocols requiring nonmaximally entangled states.

ACKNOWLEDGMENTS

G.L. acknowledges support from FONDECYT Grant No. 11085055 and Project No. PBCT-PDA21. A.C. acknowledges support from MICINN (Project No. FIS2008-05596) and the Wenner-Gren Foundation. C.S. acknowledges support from FONDECYT Grant No. 1080383.

[1] J. S. Bell, Physics (NY) **1**, 195 (1964).
[2] J. Barrett, L. Hardy, and A. Kent, Phys. Rev. Lett. **95**, 010503 (2005).
[3] L. Hardy, Phys. Rev. Lett. **68**, 2981 (1992).
[4] L. Hardy, Phys. Rev. Lett. **71**, 1665 (1993).
[5] P. H. Eberhard, Phys. Rev. A **47**, R747 (1993).
[6] J.-Å. Larsson, Phys. Rev. A **57**, 3304 (1998).
[7] D. Salart, A. Baas, C. Branciard, N. Gisin, and H. Zbinden, Nature (London) **454**, 861 (2008).
[8] S. Aerts, P. G. Kwiat, J.-Å. Larsson, and M. Zukowski, Phys. Rev. Lett. **83**, 2872 (1999); **86**, 1909 (2001).
[9] A. Cabello, A. Rossi, G. Vallone, F. De Martini, and P. Mataloni, Phys. Rev. Lett. **102**, 040401 (2009).
[10] G. Lima, G. Vallone, A. Chiuri, A. Cabello, and P. Mataloni, Phys. Rev. A **81**, 040101(R) (2010).
[11] D. Frustaglia and A. Cabello, Phys. Rev. B **80**, 201312(R) (2009).
[12] G. Vallone, P. Mataloni, and A. Cabello, Phys. Rev. A **81**, 032105 (2010).
[13] F. Sciarrino, G. Vallone, A. Cabello, and P. Mataloni, Phys. Rev. A **83**, 032112 (2011).
[14] A. Cabello, Phys. Rev. Lett. **85**, 5635 (2000); **100**, 018902 (2008).
[15] S. Goldstein, Phys. Rev. Lett. **72**, 1951 (1994).
[16] N. D. Mermin, Am. J. Phys. **62**, 880 (1994).
[17] A. Garuccio, Phys. Rev. A **52**, 2535 (1995).
[18] J. F. Clauser and M. A. Horne, Phys. Rev. D **10**, 526 (1974).
[19] J. F. Clauser, M. A. Horne, A. Shimony, and R. A. Holt, Phys. Rev. Lett. **23**, 880 (1969).
[20] D. Boschi, S. Branca, F. De Martini, and L. Hardy, Phys. Rev. Lett. **79**, 2755 (1997).
[21] M. Barbieri, F. De Martini, G. Di Nepi, and P. Mataloni, Phys. Lett. A **334**, 23 (2005).
[22] D. C. Burnham and D. L. Weinberg, Phys. Rev. Lett. **25**, 84 (1970).
[23] C. K. Hong, Z. Y. Ou, and L. Mandel, Phys. Rev. Lett. **59**, 2044 (1987).
[24] E. Santos, Found. Phys. **34**, 1643 (2004).